Available online at www.sciencedirect.com
ScienceDirect
Scripta Materialia 60 (2009) 843–846
Scripta MATERIALIA
www.elsevier.com/locate/scriptamat

The mechanical behavior and nanostructure of silica nanowires via simulations

Lilian P. Dávila,[a,*] Valerie J. Leppert[a] and Eduardo M. Bringa[b]

[a] *School of Engineering, University of California Merced, P.O. Box 2039, Merced, CA 95344, USA*
[b] *CONICET & Instituto de Ciencias Básicas, Universidad Nacional de Cuyo Mendoza, 5500 Mendoza, Argentina*

Received 21 December 2008; accepted 26 December 2008
Available online 14 January 2009

Atomistic simulations of vitreous silica nanowires under compression were evaluated for size effects on stiffness and for structural transformations using ring distributions. Results from nanowires (diameters 1.4–20.0 nm) bridge the gap between experiments and simulations. Ultrathin nanowires (diameter 4.3 nm, length 14.3 nm) show no change in structure through 25% strain. Thicker nanowires resemble bulk glass in structure and Young's modulus while longer nanowires (length ~57 nm) display buckling modes. Ultrathin nanowire results are consistent with predictions using elasticity calculations.

Keywords: Amorphous materials; Oxides; Mechanical properties; Nanostructure; Molecular dynamics simulations

The mechanical behavior of glassy systems has been studied for decades, but only recently is a detailed microscopic understanding emerging. Numerous atomistic simulations have been performed to understand the deformation of amorphous solids [1,2], metallic glasses [3,4] and oxide glasses [5–7]. In particular, the mechanical response to deformation of vitreous silica (high-purity amorphous SiO_2) has been the focus in many studies because of its technological importance and myriad of applications. Innumerable experiments conducted on this glass have produced key findings, such as an anomalous equation of state under high pressures [8,9]. We successfully reproduced the experimental pressure–volume relationships of vitreous silica under deformation using molecular dynamics (MD) simulations [7]. In that study, an elastic-to-plastic transition at a volumetric compression of ~20% was correlated with structural changes in the bulk samples determined via ring size analysis, where ring size, N, is the shortest loop formed by N Si–O bonds [7,10]. The ring size distribution in vitreous silica at ambient conditions has been shown to have an average ring size of six and the number of rings larger and smaller than six drops off sharply. High pressure can change the structure of vitreous silica and broaden this distribution [7,11]. Raman studies of compressed vitreous silica [12,13] have indicated an enhancement of distinctive lines associated with some smaller rings through particular vibration frequencies. Recently, silica nanoarchitectures based on small-membered rings have been suggested to have potential technological applications [14].

The development of structures with nanometer dimensions has raised questions about their behavior compared to bulk materials. Nanowires (NWs) have been studied in recent years due to their unique properties [15–19] and potential applications in sensors, nanoelectromechanical devices and catalysis [20]. Novel synthesis of Si, SiO_2, GaN and ZnO NWs has expanded their applications to optoelectronics, actuators and optics, making these NWs potential building blocks for nanodevices. Vitreous silica NWs have been found to possess distinct mechanical, optical and electronic properties [15–19,21,22] suitable for optical wave guiding [23], photonic devices [24] and nanofoams [25], which may be used as catalysts and low-k dielectric films.

Contemporary experiments on the mechanical properties of vitreous silica NWs are limited because of manipulation and testing challenges. Tests under resonance conditions have indicated that these NWs have a Young's modulus (E) [15] and a bending modulus [16] that are lower than those of vitreous silica fibers. Bending experiments have shown that vitreous silica NWs have elastic moduli that vary widely from the bulk material [18]. Simulations [26–29] have focused on nanomechanical studies because they can explore regimes not fully accessible experimentally. In a MD study using the BKS interatomic potential [30], the elastic modulus has been calculated under tensile loading for "bulk" vitreous silica and selected NWs [19]. The investigators have

* Corresponding author. E-mail: ldavila@ucmerced.edu

1359-6462/$ - see front matter © 2009 Acta Materialia Inc. Published by Elsevier Ltd. All rights reserved.
doi:10.1016/j.scriptamat.2008.12.057

reported $E \sim 75$ GPa for "bulk" vitreous silica, in excellent agreement with experiments, and $E \sim 85$–110 GPa for the vitreous silica NWs [19].

In this study, the mechanical behavior and ring structure of vitreous silica NWs were analyzed under uniaxial compression at room temperature. Large-scale MD simulations were conducted using the Garofalini potential [31], which is relatively efficient computationally compared with potentials with non-screened Coulomb terms, thus allowing simulations of large systems. The general approach involved creating a "bulk" glass model, carving out various solid columns from this "bulk" sample, relaxing the NWs to obtain the initial state and applying uniaxial compression. The Young's modulus of such NWs was evaluated for possible size effects and the structural changes in this material were assessed through the characteristic ring size distribution.

Several initial "bulk" glass structures were obtained [7] and solid cylinders were then carved out from the "bulk" samples, each containing from 1500 to 295,000 atoms. This method of creating NWs induced "defects" (unbonded atoms) on the lateral surface of the NWs; however, these constituted 0.1–0.5% of the NW atoms and were assumed negligible. All simulations were performed on a cubical sample ($14.3 \times 14.3 \times 14.3$ nm^3) and various cylinders ($D = 1.43$–20.05 nm, length-to-diameter L/D ratios = 0.7–10). These samples were initially equilibrated at 300 K for 0.5 ns and 1–1.9 ns, respectively, to obtain the initial state using lateral free boundary conditions for the NWs and periodic boundary conditions (PBCs) for the "bulk" sample. The forces on the atoms at both ends of our samples (last 0.2 nm) were set to zero to mimic "sample holders" to account for friction. PBCs were used along the loading z-direction for all samples. Homogeneous uniaxial compressions of the samples were performed at 300 K using a time step of 2.5 fs by: (i) rescaling the z-direction coordinates of the atoms by 0.98 (or 2% compressive strain), hence reducing the length of the sample; (ii) relaxing the sample (0.4–0.75 ns for the NWs, 0.4 ns for the "bulk" sample); and then repeating steps (i) and (ii). Such a loading scheme led to an "effective" strain rate of $\sim 10^7$ s^{-1}, smaller than previously reported [19,29]. Similar techniques have been used before to study the compression of metallic NWs [32] and vitreous silica [7]. Simulation tests were also carried out to reproduce our results. Recent studies have suggested that stress–strain curves [3] and the Young's modulus [29] are not greatly sensitive to sample preparation variations.

Since our samples were compressed only along the z-axis, the virial average stress was calculated as a function of the engineering strain. Each stress–strain σ–ε curve was evaluated using the zz component of the atomic stress σ_{zz} (average) and the relative strain along the z-direction ε_{zz}, based on the change in simulated box dimensions. A fixed volume per atom was assumed and multiplied by the number of atoms for the atomic stress calculations. Following Hooke's law ($E = \sigma/\varepsilon$), the Young's modulus was calculated from the slope in the initial linear region of each σ–ε curve by fitting a line between 0% and 6% strain. The structural variations were examined through the ring size distribution [6,7,10] using the "shortest-path" criterion [10].

Figure 1 shows the stress–strain curves of "bulk" vitreous silica and selected NWs under uniaxial compression. Our simulations produced a Young's modulus $E \sim 98.9$ GPa for the "bulk" structure which is higher than its experimental value of 75 GPa [33]. A possible reason for the overestimated E value using the Garofalini potential compared to experiments is that this potential was not explicitly fit to the experimental mechanical properties of this material, resulting in larger elastic constants, as is the case for rigid-ion potentials and a recent three-body potential [34]. Plasticity in the "bulk" glass is detected beginning at $\varepsilon \sim 0.06$ and at various strains in the NWs. Several σ–ε curves depict similar trends (bulk and NWs with $D > 5$ nm), while others are substantially different (NWs with $D = 4.3$ nm). These differences indicate that there are significant size effects on the mechanical behavior of these amorphous systems. Moreover, one NW ($D = 4.30$ nm, $L = 14.32$ nm) is found to behave as a "superelastic" sample, displaying a linear behavior in its σ–ε curve up to the largest strain reached. Unloading tests on this ultrathin NW verified this size undergoes elastic deformation. The longer NW ($L \sim 57.3$ nm) in Figure 1 also shows a superelastic-like behavior.

Most significantly, our compression simulations exhibit a distinct dependence of Young's modulus with NW diameter for the amorphous silica system, as evident in Figure 2, which includes other prior results. In this work, we deform a wide range of NW sizes ($D \sim 1.4$–20.0 nm, $L \sim 14.3$–57.3 nm). Previous work [19] reported smaller NWs ($D \sim 3.7$–6 nm) under tension. The difference in the E dependence reported here compared to prior work [19] is attributed to the different sense of stress, NW sizes and potential selected. In our study, thicker NWs ($D > 5.7$ nm) show that the elastic modulus and ring structure increasingly resemble the "bulk" sample as D increases. However, a much smaller elastic modulus is found for the NW with $D \sim 4.3$ nm, due to its unique "superelastic" behavior. The ultrathin "superelastic" NW ($D = 4.30$ nm, $L = 14.32$ nm) (Fig. 1) undergoes no change in its amorphous structure up to the highest compression simulated because it expands laterally to accommodate stresses. The radial expansion was fairly uniform along the length of this NW except for the fixed extremes, and it was consistent with a nearly constant NW volume

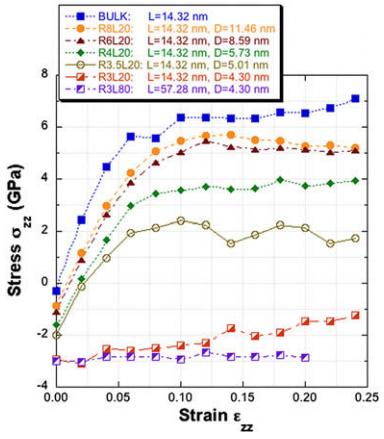

Figure 1. Virial stress vs. axial engineering strain curves for vitreous silica "bulk" and selected nanowires under uniaxial compression simulations. D and L are diameter and length, respectively. Error bars in σ_{zz} are roughly the same size as the symbols. Nanowires ($D \sim 4$ nm, $L \sim 57$ nm) are the most compliant due to buckling.

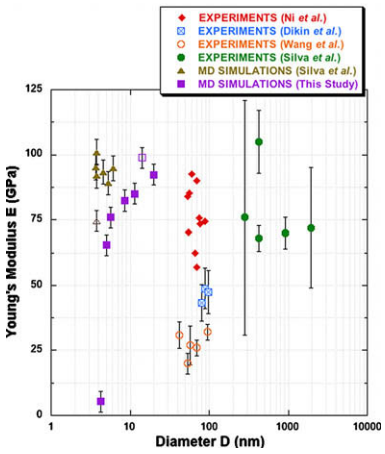

Figure 2. Young's modulus E of silica nanowires as a function of diameter D, adapted from Ref. [19]: bending experiments (◆) [18], resonance experiments (◯ ☒) [15,16], bending experiments (●) [19], MD simulations under tension (▲) and bulk silica (△) [19], and our MD simulations under compression (■) and bulk silica (□).

under deformation. In contrast, longer NWs show that buckling modes are important. Figure 3 illustrates the buckling of a long NW ($D = 4.30$ nm, $L = 57.28$ nm) at 8% strain. Note that the wavelength of the buckled surface is ~17 nm, longer than the full length of the shorter NWs ($L = 14.32$ nm). Slight buckling appears during relaxation at zero strain, and the buckling amplitude increases with strain up to our largest simulated strain (20% for this NW), without breaking of the NW. Buckling has been observed in simulations of crystalline gold NWs [35] but with a much smaller wavelength after reaching some critical strain. Our compression simulations also detect instabilities in the thinnest NWs ($D < 4.32$ nm) studied. NWs with $D \sim 2.9$ nm display surfaces that deform and reconstruct as compression increases. Other NWs ($D < 2.9$ nm) have structures that sometimes order in layers or break into clusters due to Rayleigh instabilities, which tend to break thin NWs into shorter segments [20]. The structural ordering in bulk silica was previously noted [29].

Structural transformations occurring in the glass are depicted via normalized ring size distributions, where the change in the number of rings with respect to their initial value at $\varepsilon = 0$ is plotted as a function of compression. The ring size distribution for the "bulk" glass broadens significantly at high compressions, consistent with previous findings [7,11]. Conversely, the ring structure of the "superelastic" NW ($D = 4.30$ nm, $L = 14.32$ nm) does not change. Figure 4 shows the normalized ring size distribution for (a) the "bulk" vitreous silica and (b) the "superelastic" NW at various strains. Figure 4(a) indicates the

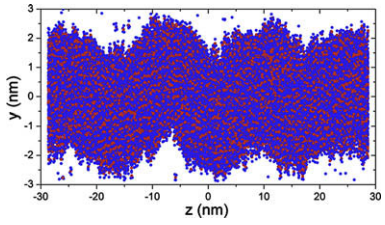

Figure 3. Buckling of a long nanowire ($L \sim 57.3$ nm, $D \sim 4.3$ nm) at a uniaxial compressive strain $\varepsilon = 0.08$, with Si atoms in red and O atoms in blue. Values y and z are the y- and z-axis coordinates respectively.

"bulk" structure is unchanged until ~6% strain, consistent with the linear region in its corresponding σ–ε curve (Fig. 1), hence the compression is elastic. Above 6% strain, an abrupt increase in the breadth of the ring size distribution is observed for the "bulk" glass, correlating with the onset of plastic compression (Fig. 1). These results are consistent with prior studies [7]. Figure 4(b) confirms that the structure of a "superelastic" NW ($D = 4.30$ nm, $L = 14.32$ nm) remains unchanged, with no detectable "plasticity" up to the highest strain simulated. This absence of plasticity leads to the "barreling" of the NW while keeping its volume constant. Ring analysis of a longer NW (Fig. 3) ($L = 57.28$ nm) shows similar results.

Further analysis of Figure 1 indicates that our initial NWs show nonzero stresses, as observed in compression simulations of crystalline silica nanorods [29] and gold nanopillars [36]. The origin of the initial nonzero stresses has been attributed in metallic nanopillars to surface stresses and found to be dependent on NW size [36]. Nonzero stresses may also result from structures not being fully equilibrated, but this is unlikely to be the case for our NWs since an extensive relaxation phase was used to obtain the initial states. The "superelastic" behavior of the ultrathin NWs is possibly due to surface stress effects, which are expected to dominate nanomaterials, as described by analytical models [37,38]. Using elasticity theory, researchers recently showed that surface effects on the elastic modulus of NWs are especially significant when D is a few nanometers in size [37]. That study even estimated a critical NW size of $D \sim 4$ nm for silica, with ~30% smaller stiffness than the bulk, in good agreement with our ultrathin NWs (Fig. 1). The authors also predicted that thin silica NWs will have attenuated elastic moduli under compression, consistent with our findings (Fig. 2). The increase in stiffness of NWs as diameter decreases under tension, reported before [19], is also in good agreement with such predictions [37]. Therefore, our results together with Ref. [19] agree with the unique mechanical behavior of thin NWs predicted earlier. Namely, as NWs decrease in diameter they become more compliant under compression but stiffer under tension. This mechanical response of the NWs is contrary to the behavior of bulk vitreous silica, typically stiffer under compression [33]. The results in the intermediate region ($10 < D < 100$ nm) in Figure 2 are especially important for understanding the various elastic moduli reported in NWs with $D < 100$ nm and for predicting results. Figure 2 also infers that simulations will soon provide a wider range of predictions for practical NW sizes. This will allow the rational exploration of different experimental conditions, NW geometries and assemblage of superstructures.

Our results also show that the differences in the ring distribution in the bulk and NWs are due to differences in densities, as shown before [7]. Extrapolating our results (Fig. 2), we predict E will not vary significantly for experimental NW sizes ($50\text{ nm} < D < 100$ nm), roughly consistent with bending experiments [18,19] but not with resonance experiments [15,16]. The structures in our study represent ideal high-purity amorphous samples under vacuum conditions. Experimental NWs will likely contain defects (e.g. cracks), impurities (e.g. water) and even coatings [39], all of which will affect their mechanical properties.

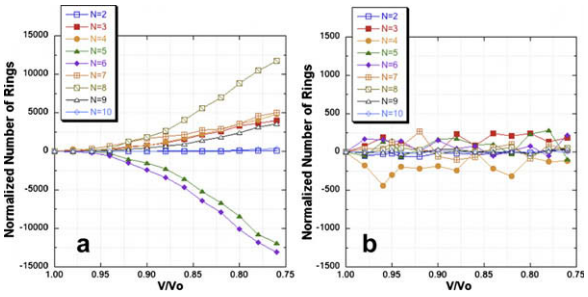

Figure 4. Normalized ring size distribution for (a) "bulk" sample and (b) a nanowire ($L \sim 14.3$ nm, $D \sim 4.3$ nm) as a function of volume V, where V_0 is the initial uncompressed volume. N describes an N-membered ring (e.g. $N = 10$ indicates a 10-membered ring). The normalization in the vertical axis represents the number of rings of size N over the initial total number of rings in the model. The nanowire in (b) shows very small ring variations.

In summary, the mechanical behavior and structure of vitreous silica NWs and bulk are investigated under uniaxial compression simulations at 300 K. The "bulk" glass depicts a σ–ε curve with regimes corresponding to changes in its ring size distribution. The NWs respond differently depending on their diameter. For thin NWs ($4\text{ nm} < D < 20\text{ nm}$) under compression, the elastic moduli decrease with decreasing diameter for strain rates $\sim 10^7\ \text{s}^{-1}$. In addition, a superelastic response is observed for a NW with $D \sim 4$ nm, which does not change in structure up to the highest strain simulated. Longer NWs ($L \sim 57$ nm) with similar diameter exhibit buckling and no detectable structural transformations. The thinnest NWs ($D < 4$ nm) show structural instabilities while thicker NWs ($D > 5$ nm) increasingly resemble the "bulk" glass. Our modeling efforts are consistent with recent independent research [37] which, along with other theoretical studies [36,38], attribute the mechanical behavior of thin NWs to dominant surface stress effects. The success of future manufacturing efforts using such NWs will depend on understanding their properties, with implications for self-assembly and nanomanipulation processes. Most significantly, our MD results using silica NWs could be applied to silica nanofoams similar to those recently studied [25], in the same way that simulations of gold NWs were applied to gold nanofoams [40]. Specifically, our research can help understand nanoscale silica foams and nanoporous self-assembled silica structures that can potentially be used in a large number of applications. Thus far, although novel technology has been used to produce silica NWs under different conditions, advances in specialized equipment and testing methods will be needed to fully characterize these nanostructures.

The authors thank M.-J. Caturla, S.H. Garofalini, J.F. Shackelford, A. Caro, L.A. Zepeda-Ruiz and J. Marian for fruitful discussions, and A. Kubota for the ring code. LPD was supported by the UC President's Postdoctoral Fellowship program. This work was performed under the auspices of the U.S. Department of Energy by Lawrence Livermore National Laboratory under Contract DE-AC52-07NA27344.

[1] M.L. Falk, J.S. Langer, Phys. Rev. E 57 (1998) 7192.
[2] C.A. Schuh, A.C. Lund, Nat. Mater. 2 (2003) 449.
[3] F. Shimizu, S. Ogata, J. Li, Acta Mater. 54 (2006) 4293.
[4] N.P. Bailey, J. Schiøtz, K.W. Jacobsen, Phys. Rev. B 73 (2006) 064108.
[5] W. Jin, R.K. Kalia, P. Vashishta, J.P. Rino, Phys. Rev. Lett. 71 (1993) 3146.
[6] J.P. Rino, G. Gutierrez, I. Ebbsjo, R.K. Kalia, P. Vashishta, MRS Proc. 408 (1996) 333.
[7] L.P. Dávila, M.-J. Caturla, A. Kubota, B. Sadigh, T. Díaz de la Rubia, J.F. Shackelford, S.H. Risbud, S.H. Garofalini, Phys. Rev. Lett. 91 (2003) 2055011.
[8] W. Primak, Compacted States of Vitreous Silica – Studies of Radiation Effects in Solids, Gordon & Breach, New York, 1975.
[9] H. Sugiura, R. Ikeda, K. Kondo, T. Yamadaya, J. Appl. Phys. 81 (1997) 1651.
[10] A. Kubota, M.-J. Caturla, J.S. Stolken, M.D. Feit, Opt. Express 8 (2001) 611.
[11] L.P. Davila, S.H. Risbud, J.F. Shackelford, in: Ceramic and Glass Materials: Structure, Properties and Processing. Springer, NewYork, 2008, p. 73.
[12] S.G. Demos, L. Sheehan, M.R. Kozlowski, Int. Soc. Opt. Eng. 3933 (2000) 316.
[13] J.W. Chan, T. Huser, S. Risbud, D.M. Krol, Opt. Lett. 26 (2001) 1726.
[14] D. Zhang, R.Q. Zhang, J. Phys. Chem. B 110 (2006) 15269.
[15] Z.L. Wang, R.P. Gao, P. Poncharal, W.A. de Heer, Z.R. Dai, Z.W. Pan, Mater. Sci. Eng. C 16 (2001) 3.
[16] D.A. Dikin, X. Chen, W. Ding, G. Wagner, R.S. Ruoff, J. Appl. Phys. 93 (2003) 226.
[17] L. Tong, J. Lou, Z. Ma, Proc. SPIE 6029 (2005).
[18] H. Ni, X. Li, H. Gao, Appl. Phys. Lett. 88 (2006) 043108.
[19] E.C.C.M. Silva, L. Tong, S. Yip, K.J. Van Vliet, Small 2 (2006) 239.
[20] Y.N. Xia, P.D. Yang, Y.G. Sun, Y.Y. Wu, B. Mayers, B. Gates, Y.D. Yin, F. Kim, H. Yan, Adv. Mater. 15 (2003) 353.
[21] Y. Hao, G. Meng, C. Ye, L. Zhang, Appl. Phys. Lett. 87 (2005) 0331061.
[22] G. Bilalbegović, J. Phys. 18 (2006) 3829.
[23] L. Tong, J. Lou, E. Mazur, Opt. Express 12 (2004) 1025.
[24] L. Tong, E. Mazur, J. Non-Cryst. Solids 354 (2008) 1240.
[25] H. Fan, C. Hartshorn, T. Buckheit, D. Tallant, R. Assink, R. Simpson, D.J. Kissel, D.J. Lacks, S. Torquato, C.F. Brinker, Nat. Mater. 6 (2007) 418.
[26] H. Liang, M. Upmanyu, H. Huang, Phys. Rev. B 71 (2005) 241403.
[27] J. Diao, K. Gall, M.L. Dunn, Nano Lett. 4 (2004) 1863.
[28] M.I. Haftel, K. Gall, Phys. Rev. B 74 (2006) 035420.
[29] E.C.C.M. Silva, J. Li, D. Liao, S. Subramanian, T. Zhu, S. Yip, J. Comput-Aid. Mater. Des. 13 (2006) 135.
[30] B.W.H. van Beest, G.J. Kramer, R.A. van Santen, Phys. Rev. Lett. 64 (1990) 1955.
[31] E.B. Webb, S.H. Garofalini, J. Chem. Phys. 101 (1994) 10101.
[32] J. Diao, K. Gall, M.L. Dunn, J.A. Zimmerman, Acta Mater. 54 (2006) 643.
[33] B. Bhushan, Handbook of Nanotechnology, Springer, Berlin, 2004.
[34] L. Huang, L. Duffrène, J. Kieffer, J. Non-Cryst. Solids 349 (2004) 1.
[35] J. Marian, J. Knap, Int. J. Multiscale Comput. Eng. 5 (2007) 287.
[36] E. Rabkin, H.-S. Nam, D.J. Srolovitz, Acta Mater. 55 (2007) 2085.
[37] M.R. Shankar, A.H. King, Appl. Phys. Lett. 90 (2007) 1419071.
[38] R.C. Cammarata, K. Sieradzki, Annu. Rev. Mater. Sci. 24 (1994) 215.
[39] Y. Qu, R. Porter, F. Shan, J.D. Carter, T. Guo, Langmuir 22 (2006) 6367.
[40] J. Biener, A.M. Hodge, J.R. Hayes, C.A. Volkert, L.A. Zepeda-Ruiz, A.V. Hamza, F.F. Abraham, Nano Lett. 6 (2006) 2379.